NURETH14-042

DERIVATION OF A LOOK-UP TABLE FOR TRANS-CRITICAL HEAT TRANSFER FOR WATER-COOLED TUBES

H. Zahlan, D.C. Groeneveld and S. Tavoularis
University of Ottawa, Ottawa, Ontario, Canada

Abstract

A trans-critical look-up table (LUT) provides predictions of heat transfer for the region near and beyond the critical point for water. The trans-critical LUT starts at the high subcritical pressure of 19 MPa and extends to supercritical pressures, up to 30 MPa. The intended range of application of the LUT is sufficiently wide to fit all conditions for which conventional single-phase correlations do not apply. This article describes the progress made in deriving a trans-critical LUT for tubes cooled by vertical upflow of high-pressure water.

The University of Ottawa (UO) team has compiled a large trans-critical water database and combined it with supercritical water (SCW) databases from other organizations. The expanded database has been carefully examined and duplicate data as well as obvious outliers and data not satisfying a heat balance have been removed. The expanded UO database includes more than 25,000 screened data points.

A literature review has been performed in parallel with the LUT compilation and has identified 18 single-phase, near-critical and supercritical (SC) heat transfer correlations. The predictions of these correlations have been compared to the experimental values of the UO expanded database and a statistical error analysis of the comparison results has been performed. The parametric trends of the uncertainty of the more promising correlations are described in this paper.

A skeleton LUT has been constructed in which the heat transfer coefficients are assumed to be unique functions of pressure, mass flux, heat flux (or surface temperature) and fluid enthalpy; the LUT domain has been subdivided into sub-domains, each associated with a distinct heat transfer mechanism. The sub-domains include high pressure subcritical regions (liquid, subcritical vapor, and subcritical two-phase regions), SC regions (high-density state or SC liquid-like region, and low-density state or SC vapor-like region) and a near-critical or near-pseudo-critical region. For each region, the best correlations were identified and subsequently used for the construction of the skeleton LUT, which will be updated by experimental data suitably normalized. The parametric trends of the skeleton table have been examined and compared to experimental data.

Introduction

The Supercritical Water-Cooled Reactor (SCWR) is one of the most promising candidates for the next generation of nuclear power reactors. Research into the thermalhydraulics of SCWR has therefore become an active field. Reliable supercritical heat transfer (SCHT) prediction methods are required for the thermal design and safety analysis of the SCWR.

Near the critical point, fluids encounter very large changes in their thermo-physical properties; such changes become smaller at lower subcritical pressures and at higher supercritical pressures away from the pseudo-critical point. Because of these large changes, trans-critical heat transfer coefficients are difficult to predict. In the literature more than 20 correlations are available for predicting the heat transfer in this region, most of which are of the Dittus-Boelter (1930) equation type. In general, these correlations do not account for improvement or deterioration in heat transfer near the critical point. Some of the most recent correlations, based on water data, attempt to consider the effect of enhancement and deterioration near the critical point at SCHT conditions, but a simple correlation cannot be expected to describe the normal, improved and deteriorated heat transfer. The near-critical heat transfer mode can also be affected by flow orientation, geometry and flow conditions.

The objective of this work is to derive a trans-critical heat transfer LUT, which will cover a wide range of flow conditions, therefore overcoming the range-of-validity-limitation associated with current correlations. In addition, this trans-critical LUT will include the high-pressure subcritical region and will thus provide the transition from the subcritical into the SC region.

1. Trans-critical heat transfer database

The UO team has compiled a large subcritical and SC database (Groeneveld and Zahlan, 2009; Zahlan et al., 2010). This database included data for water and other fluids and different geometries. Additional water datasets, tabulated and/or identified by Lowenberg et al. (2005, 2008; University of Stuttgart), and by Cheng (2009; Shanghai JiaoTong University) have been included in the expanded UO trans-critical heat transfer database. Recently, UO received an additional SCHT water database compiled at the University of Ontario Institute of Technology (UOIT) containing 10479 SCHT data points (Pioro, 2010). The main contributor to the UOIT database for vertical upflow of water in circular tubes is Kirillov et al. (2005), whose datasets were found to include data previously reported by other organizations. The UOIT database was subjected to a careful review, heat balance checks and screening for duplicates and obvious outliers. Table 1 shows a summary of the 2010 SCHT water data compilations from different sources. Details about the parameter ranges for all datasets from all sources were presented by Zahlan et al. (2011). Some of these datasets were extracted from graphs using data digitization software which introduces additional uncertainties (Zahlan et al., 2010). Frequently, more than one set of SCHT dataset covers similar flow conditions; this will enhance the reliability of the LUT for these conditions.

1.1 Supercritical sub-regions

At an earlier stage of this research, depending on wall temperature T_w, bulk fluid temperature T_b and pseudo-critical temperature T_{pc}, the SCHT data were classified into three distinctive SC sub-regions: (i) a high density state (liquid-like) region ($T_w < T_{pc}$ and $T_b < T_{pc}$), (ii) a near-critical or near-pseudo-critical region ($T_{pc} < T_w$ and $T_b < T_{pc}$), and (iii) a low density state (gas-like) region

(T_{pc} < T_w and T_{pc} < T_b). This classification was meant to take into account the distinct heat transfer mechanisms that apply within each sub-region. However, this approach did not consider the fact that the thermo-physical properties change significantly within a range of temperatures near the pseudo-critical value. Therefore, it was decided to redefine the boundaries of the near-critical/pseudo-critical region by introducing a narrow range of temperatures $T_{pc} - \Delta T < T < T_{pc} + \Delta T$, within which the thermo-physical properties change significantly. It was found that this range was described fairly well for different pressures by the empirical relationship $\Delta T/T_{pc} = 3.1\times10^{-3}(P/P_c)$, in which the pressure is normalized based on the critical pressure P_c and the numerical values of all temperatures are in degrees K. In the current work, each SCHT data point was classified into one of these three redefined sub-regions: (i) high density state (liquid-like) region (T_w, $T_b < T_{pc} - \Delta T$), (ii) near-critical or near-pseudo-critical region ($T_{pc} - \Delta T < T_w$ and $T_b < T_{pc} + \Delta T$), and (iii) low density state (gas-like) region ($T_{pc} + \Delta T < T_w$, T_b).

1.2 Data screening

The method for screening the data for duplicates (runs and points between different datasets and within a dataset), obvious outliers and data that did not agree with a simple heat balance was presented by Zahlan et al. (2010).

2. Assessment of heat transfer prediction methods

Different single-phase and SCHT correlations were applied to the UO subcritical and SC expanded databases (Zahlan et al., 2010). The UO assessment covered a large number of correlations, including the most recent ones, which were published in 2009-2010. These correlations were described and tabulated by Zahlan et al. (2011). Twelve SCHT correlations and four single-phase correlations have been applied to the expanded UO database, including the new compilation from UOIT. The overall average error e_A and the root mean square error e_{RMS} were calculated for all correlations.

Table 2 compares the average and rms errors for all correlations in the three SC regions. This table shows that the Mokry et al. (2008) correlation has the lowest e_{RMS} in the three SCHT regions. The distributions of average and rms errors for the best correlations, including the one by Mokry et al. (2008), with respect to Re_b, $Pr_{avg,b}$, P/P_c and D, were presented by Zahlan et al. (2010, 2011) in the form of plots for the three SC regions for the combined UO/SJTU/US/UOIT database. Table 3 shows percentages of all combined data predicted by the most promising correlations within an error band of ±10% (e_{10}), ±20% (e_{20}), ±30% (e_{30}), and ±50% (e_{50}).

Zahlan et al. (2010) showed that this correlation presented the lowest rms error when applied to UO combined high-pressure subcritical superheated-steam data. In addition, for single-phase liquid heat transfer, the correlation of Gnielinski (1976) showed the best agreement with the UO combined high-pressure subcritical water data.

An error analysis has also been performed on each dataset in the three SC regions. The average error, rms error and percentage of data for the four error bands were calculated for each dataset. Details of the results were tabulated by Zahlan et al. (2011).

3. Derivation of the trans-critical look-up table

The derivation of a reliable heat transfer prediction method ideally requires a database which covers all conceivable conditions that can be encountered in a SCWR during normal and abnormal operation. The derivation of a look-up table requires first the construction of a skeleton table to provide the initial estimate of the heat transfer coefficient (*HTC*) values at discrete points of the most important independent flow parameters: pressure *P*, mass flux *G*, coolant enthalpy H_b and temperature difference T_w-T_b between wall and bulk flow[1]. The *HTC* values of the skeleton table were based on predictions from reliable heat transfer correlations, whose uncertainty has been assessed as described in Section 2.

To improve the prediction accuracy of the current skeleton look-up table, the skeleton table values will be modified using the data from the combined UO databank. Zahlan et al. (2010) described the screening process that was used to select the 24253 trans-critical heat transfer data from a database containing a total of 36030 data points (Table 1). The selected data will be normalized with respect to the adjacent grid conditions (*P, G,* H_b and T_w-T_b) and the reference table diameter of 8 mm using procedures similar to those used by Groeneveld et al. (2003) in deriving the film boiling LUT (2003 FB-LUT).

The LUT is not expected to be smooth and will likely display an irregular variation (i.e., devoid of physical basis) with *P, G,* H_b and T_w-T_b. These fluctuations are attributed to data scatter, systematic differences between different datasets, and possible effects of secondary parameters such as heated length, surface conditions, flow instability etc. Sharp variations in heat transfer coefficient will also likely be observed at boundaries between regions where experimental data are available and regions where correlations or other approaches need to be employed and at the transition to subcritical prediction methods for film boiling (FB), critical heat flux (*CHF*) or single phase heat transfer. Note that predictions at conditions for which no data are currently available are expected to be complex and require a mechanistic understanding of SCHT, including near-wall phenomena. This also requires a close examination of the LUT trends vs. *P, G,* H_b and T_w-T_b at conditions closest to those of the missing data.

To minimize unrealistic sudden transitions (i.e., transitions which are not based on experimental trends), the smoothing procedure developed by Huang and Cheng (1994) will be applied. The smoothing procedure will not be applied at conditions near the pseudo-critical point where rapid changes in *HTC* are expected to be present.

The trans-critical LUT domain spans the complete range of flow conditions of interest; Table 4 presents the proposed range of parameters and grid points of the trans-critical LUT. Because of the limitations in the database coverage, some of the LUT values will have to be based on existing heat transfer correlations and/or extrapolations from the database.

Two other parameters that could have a significant effect on heat transfer are the tube inside diameter and the flow direction. The diameter effect appears to have a slight negative effect on the *HTC* ($HTC \sim D^{-0.1}$ to $D^{-0.2}$) as predicted by the SCHT correlations, the single phase heat transfer correlations and the 2003 FB-LUT, but could have a more significant effect in the

[1] Instead of the wall superheat T_w-T_b, the heat flux *q* could be used as an independent parameter.

deteriorated and enhanced heat transfer region. Because of the limited availability of SCHT data covering a wide range of diameters, and because most of the data are available within the diameter range of 5–10 mm, it was decided to construct the skeleton LUT for a diameter of 8 mm and investigate the optimum form of the diameter correction factor once the trans-critical LUT has been finalized.

Considering that the large majority of the SCHT and high pressure subcritical heat transfer tube data were obtained for vertical upflow, the skeleton table (and subsequent trans-critical LUT) will be constructed for vertical upflow. Corrections for flow direction (downflow, horizontal flow, inclined flow) may be derived after completing the trans-critical LUT for conditions where mixed convection is important as evidenced by the presence of heat transfer enhancement/deterioration.

4 Skeleton table derivation

The trans-critical heat transfer skeleton table is based on the combination of two tables: (i) a skeleton table for the subcritical high-pressure region and (ii) a skeleton table for the SCHT region. The following sections will describe the methodology used in the derivation of these two skeleton tables and the applied heat transfer prediction methods.

4.1 Subcritical skeleton table

This table covers discrete pressures between 19 and 22 MPa, at increments of 1 MPa. Heat transfer in the subcritical single-phase and two-phase regions has been investigated thoroughly and the recommended heat transfer prediction methods are fairly accurate. The 2003 FB-LUT has been chosen for the prediction of heat transfer in this region for the pressures P = 19 and 20 MPa. However, as presented in Table 5, the parameter range of the 2003 FB-LUT (Groeneveld et al., 2003) and this skeleton table do not overlap well. Therefore, the 2003 FB-LUT was extended to cover a much wider quality (or bulk enthalpy) range; this extension is partially based on the trends of the single-phase heat transfer correlations and the change in heat transfer modes depending on the value of the wall temperature in the nucleate boiling region, at the *CHF* point and at the minimum film boiling point (MFB).

As mentioned previously, the trans-critical LUT presents the dependent parameter *HTC* as a function of four independent parameters: P, G, ΔT_w and H_b for upflow of water inside an 8 mm tube. Each of the table grid points should be correctly associated with the corresponding heat transfer mode; the method to make this association is based on a comparison with the boundaries for each heat transfer mode as can be determined from standard heat transfer maps or flow boiling curves. Having determined the appropriate heat transfer mode, the corresponding *HTC* is predicted using best available correlations for each region. The method for estimating the *HTC* starts from comparing T_w and the corresponding saturation temperature T_{sat} at the table pressure. The *CHF* and minimum film boiling points are transition points on the boiling curve. The corresponding prediction methods for each heat transfer mode of the boiling curve are as follows.

Methodology for estimating HTC:

(i) *Single-phase heat transfer* ($T_w < T_{sat}$): the Gnielinski (1976) correlation was applied for single-phase forced convection heat transfer to water.

(ii) *Nucleate boiling (NB) region*[2] ($T_{sat} < T_w < T_{CHF}$): if $T_{sat} \leq T_w$, then find the corresponding *CHF* from the 2005 CHF-LUT[3] and compare T_w with T_{CHF} (obtained by the correlation of Thom et al., 1965). If $T_w < T_{CHF}$, the nucleate boiling heat flux q_{NB} is calculated using the Thom et al. (1965) correlation. Next, q_{NB} is compared to $q_{single\text{-}phase}$, where $q_{single\text{-}phase} = h_{single\text{-}phase} \times (T_w - T_b)$ and $h_{single\text{-}phase}$ is the heat transfer coefficient predicted by the single-phase correlation of Gnielinski (1976); the higher heat flux between q_{NB} and $q_{single\text{-}phase}$, i.e., max (q_{NB}, $q_{single\text{-}phase}$) will correspond to the correct heat transfer mode.

(iii) *Transition boiling region*: transition boiling (TB) occurs when $T_{MFB} > T_w > T_{CHF}$, where the minimum film boiling point represents the transition between TB and film boiling. T_{MFB} is predicted following Groeneveld and Stewart (1982) for $P > 9000$ kPa. To find the transition boiling heat flux, a linear interpolation on log-log scale of q vs. ΔT_w is recommended (Groeneveld et al., 1986), as predicted by the following two equations

$$q_{TB} = q_{MFB}\,(CHF/q_{MFB})^{m} \tag{1}$$

where

$$m = ln\frac{(T_{MFB} - T_{sat})}{(T_{w,TB} - T_{sat})} \Bigg/ ln\frac{(T_{MFB} - T_{sat})}{(T_{CHF} - T_{sat})} \tag{2}$$

and q_{MFB} is obtained by applying the Mokry et al. (2008) correlation (described below) based on film temperature for *HTC*.

(iv) *Post-CHF heat transfer:* this region includes film boiling and single-phase forced convection heat transfer to superheated steam and corresponds to $T_{MFB} \leq T_w$. For $P \leq 20$ MPa, the 2003 FB-LUT was applied for the prediction of *HTC* for $-0.2 \leq X_{th} \leq 2$. For $X_{th} < -0.2$ and for pressures and wall temperatures in the range of applicability of the 2003 FB-LUT, it was assumed that *HTC* remains constant with decreasing thermodynamic quality below -0.2. For $X_{th} > 2$, the Mokry et al. (2008) correlation

$$\mathrm{Nu}_b = 0.0061\,\mathrm{Re}_b^{0.904}\,\mathrm{Pr}_{avg}^{0.684}\left(\frac{\rho_w}{\rho_b}\right)^{0.564} \tag{3}$$

was applied, where the average Prandtl number Pr_{avg} is based on the average C_p.

---

[2] Forced convection instead of nucleate boiling may be present, but because the values of $T_w - T_{sat}$ for these heat transfer modes are similar and very small (typically < 1 K), the simpler correlation (Thom et al., 1965) is used for nucleate boiling.

[3] To predict the *CHF* outside the 2005 CHF-LUT range, the following assumptions are made:
- For P = 21, 22 MPa and $X_{th} < -0.5$: *CHF* is assumed constant, i.e. $CHF_{X<-0.5} = CHF_{X=0.5}$
- For P = 22 MPa: *CHF* is assumed equal to half of the corresponding *CHF* at P = 21 MPa

Post-CHF heat transfer for P = 21 and 22 MPa: for the region $X_{CHF} < X_e < 1.0$, the *HTC* is predicted from

$$\text{Nu}_{\text{film}} = 0.0061\,\text{Re}_{\text{b, two phase}}^{0.904}\,\text{Pr}_{\text{avg, film}}^{0.684}\left(\frac{\rho_w}{\rho_b}\right)^{0.564} \quad (4)$$

where Re_b is replaced by the homogeneous $\text{Re}_{\text{b,two phase}} = \frac{GD}{\mu_{\text{film}}}\left(x_e + (1 - x_e)\frac{\rho_g}{\rho_f}\right)$,

$\text{Pr}_{\text{avg, film}} = \frac{C_{\text{p,avg}}\,\mu_{\text{film}}}{k_{\text{film}}}$ and $C_{\text{p,avg}} = \frac{H_w - H_b}{T_w - T_{sat}}$, Equation (4) is applied for $X_{CHF} < X_{th} < 1.0$, where $q_{MFB} = h_{Eqn.(4)}\,(T_{MFB} - T_{sat})$.

- Film boiling occurs when $T_w > T_{MFB} > T_{CHF}$; here Equation (4) is used based on film temperature and the homogenous two-phase Reynolds number (described above).
- Superheated steam region: when $X_{th} > 1.0$, film boiling is assumed no longer present and Equation (4) converges into Equation (3), based on bulk temperature and Re_b.

Table 6 shows a section of the subcritical part of the skeleton table at *P* = 21000 kPa, *G* = 1000 kg/m^{2}s and T_w-T_b = 10 to 100 K. Note that the *HTC* of the look-up table is always with respect to the bulk temperature, i.e., $h_{LUT} = q / (T_w - T_b)$ where $T_b = T_{sat}$ only for $0 < X_{th} < 1$.

4.2 Supercritical skeleton table

As described in Section 2, the Mokry et al. (2008) equation showed the best agreement with the expanded SCW databank. Equation (3) has been applied in the three SCHT regions. In the derivation of Equation (3), Mokry et al. (2008) removed heat transfer data typical of deterioration or enhancement of SCHT. Therefore, the resulting skeleton table does not include deterioration and enhancement of SCHT but these effects will be included when the skeleton table is updated with experimental values.

4.3 Parametric trends of the trans-critical skeleton table

Figure 1 shows the boiling curves predicted by the heat transfer logic described in Section 5.1 and used for constructing the skeleton table. The correlations described in Section 4.1 were applied in the construction of these boiling curves. The first plot on Figure 1 shows a family of boiling curves at *G* = 1000, *X* = 0.2 for the table pressure range (*P* = 19 to 22 MPa). With increasing pressure, the nucleate boiling curves become closer to the transition boiling curves. *CHF* decreases with increasing pressure, because of the significant reduction in latent heat of vaporization when approaching the critical pressure. Here the wall superheats become smaller compared with similar boiling curves at lower pressure. This results in a very fast transition from single phase heat-transfer to water to post-dryout or superheated steam cooling. The second plot of Figure 1 shows a set of boiling curves for different mass velocities at *P* = 21 MPa. With increasing *G*, *CHF* and q_{MFB} increase. The third plot in this figure shows the variations in the boiling curve with increasing X_{th} (0, 0.2, 0.5 and 1) at *P* = 21 MPa. On this figure, *CHF* decreases with increasing X_{th}; however at X_{th} = 1, the two phase region disappears and no *CHF* can occur, as this point is the start of superheated steam region.

Figure 2 shows the parametric trends of the skeleton table with respect to some of the independent LUT parameters. Figure 2-(a) presents the variation of *HTC* for P = 21 MPa, G = 1000 kg/m^{2}s and D = 8 mm. The *HTC* varies with changing T_w-T_b and H_b. *HTC* increases with an increase in H_b and a decrease in T_w-T_b. The smaller T_w-T_b correspond to the nucleate boiling heat transfer mode that has *HTC* values considerably higher than those corresponding to single-phase convection heat transfer. Figure 2-(b) illustrates the *HTC* increase with an increase in mass velocity from 100 to 5000 kg/m^{2}s as predicted again by the single-phase convection and film boiling heat transfer prediction methods. Similarly, Figure 2-(c) shows *HTC* variations with an increase in pressure from 19 to 22 MPa; *HTC* increases slightly at the beginning and sharply at P = 22 MPa, due to enhanced thermo-physical properties of both liquid and vapor as the fluid approaches the critical point. Figure 2-(d) shows a smooth trend of increase of *HTC* with an increase in G and a decrease in T_w-T_b for P = 21 MPa, D = 8 mm and H_b = 2000 kJ/kg.

Figure 3 presents comparisons of the experimental data of Schmidt (1959) and the predictions of the skeleton table at similar flow conditions. The Schmidt (1959) data correspond to a wide range of fluid enthalpy, so that different heat transfer modes were present. Figure 3a shows the subcritical heat transfer data and skeleton table predictions for $P \approx$ 20.3 MPa, G = 700 kg/m^{2}s, $D \approx$ 5 mm). As expected, the trend of the skeleton table prediction is comparable to the corresponding trend of the Schmidt data. Figure 3b shows a similar comparison, but at a SC pressure, $P \approx$ 25.3 MPa, G = 700 kg/m^{2}s, $D \approx$ 5 mm. Here the agreement between the Schmidt data and the skeleton table is less noticeable. This is partially attributed to the use of Equation (3) for the construction of the SC part of the skeleton table. As mentioned in the previous section, this equation does not consider enhanced and deteriorated heat transfer; therefore, the peak points shown by the Schmidt data in Figure 3-(b) could not be predicted by this skeleton table. Although enhanced and deteriorated heat transfer is not predicted, the general trend of variations of ΔT_w vs. H_b is maintained.

5. Summary and concluding remarks

A thorough assessment of all leading single-phase and SCHT correlations has been performed and the most promising correlations have been selected for the construction of the trans-critical LUT.

The heat transfer logic used for determining the relevant heat transfer modes has been presented for the high-pressure subcritical region.

A skeleton table for the high subcritical pressure and supercritical heat transfer has been generated; the 2003 FB LUT and 2005 CHF-LUT as well as various heat transfer correlations have been employed in the derivation of this skeleton table.

The parametric trends of the skeleton table have been verified against boiling curve and experimental data.

Nomenclature

D	tube inside diameter	(mm, m)
G	mass flux	(kg m^{-2} s^{-1})
H	enthalpy	(kJ kg^{-1})
P	pressure	(kPa)
q	heat flux	(kW m^{-2})
T	temperature	(˚C or K)
e	error	(%)
e_{10}, e_{20}, etc	% of data within specified error range	(± 10%, ± 20% etc.)

Subscripts

b	bulk
c	critical
pc	pseudo-critical
w	wall
A	average
RMS	root mean square

Dimensionless numbers

Re	Reynolds number	$(= G\,D\,\mu^{-1})$
Pr	Prandtl number	$(=\mu C_p/k)$
Pr_{avg}	averaged or modified Prandtl number	$(= (H_w-H_b)\mu_b\,/\,(k_b\times(T_w-T_b)))$

Abbreviations

CP	critical point
SCW	supercritical water
SCHT	supercritical heat transfer
HTC	heat transfer coefficient

6. References

Bishop, A.A., Sandberg, R.O., and Tong, L.S., "Forced convection heat transfer to water at near-critical temperatures and supercritical pressures", *A.I.Ch.E.-I.Chem.E Symposium Series No*. 2, 1965, pp. 77−85

Cheng, X., 2009, Private communication

Cheng, X., Yang, Y.H., and Huang, S.F., "A simple heat transfer correlation for SC fluid flow in circular tubes", NURETH-13, Kanazawa City, Ishikawa Prefecture, Japan, September 27-October 2, 2009

Dittus, F.W., and Boelter, L.M.K., University of California, Berkeley, Publications on Engineering, Vol. 2, 1930, pp. 443–461

Gnielinski, V., "New equation for heat and mass transfer in turbulent pipe and channel flow", *Intern. Chem. Eng.*, Vol. 16, No. 2, 1976, pp. 359–366

Griem, H., "A new procedure for the at near-and supercritical prediction pressure of forced convection heat transfer", *Heat Mass Trans.*, Vol. 3, 1996, pp. 301–305

Groeneveld D.C. and Snoek, C., "A Comprehensive examination of heat transfer correlations suitable for reactor safety analysis", *Multiphase Science & Tech.*, Vol. 2, 1986, pp. 181-274

Groeneveld, D.C., and Zahlan, H.Z., "SCWR data compilation and LUT", Progress Report to AECL, December 31, 2009

Groeneveld, D.C. and Stewart, J.C., "The minimum film boiling temperature for water during film boiling collapse", Proceedings of the 7th IHTC, Munich, FRG, Vol. 4, 1982, pp. 393-398

Groeneveld, D.C., Shan, J.E., Vasic, A.Z., Durmayaz, A., Yang, J., Cheng, S.C., and Tanase, A., "The 2005 CHF Look-up table", log166, NURETH-11, Avignon, France, 2005 October 2−6

Groeneveld, D.C., Leung, L.K.H., Vasic, A., Guo, Y.J., and Cheng, S.C., A Look-up table for fully developed film-boiling heat-transfer, *NED*, Vol. 225, 2003, pp. 83–97

Gupta, S., Mokry, S., Farah, A., King, K., Peiman, W., and Pioro, I., "Developing a heat-transfer correlation for supercritical-water flow in bare vertical tubes and its application", 2010 UOIT unpublished report

Hadaller, G., and Banerjee, S., "Heat transfer to superheated steam in round tubes", AECL Report, 1969

Huang, X. C., and Cheng, S. C., "Simple method for smoothing multidimensional experimental data with application to the CHF and PDO look-up table, *Numer. Heat Trans.*, Part B, Vol. 26, 1994, pp. 425– 438

Jackson, J. D., "Consideration of the heat transfer properties of supercritical pressure water in connection with the cooling of advanced nuclear reactors", Proc. of the 13th Pacific Basin Nuclear Conference Shenzhen City, China, 2002

Kirillov, P., Pometko, R., Smirnov, A. et al., "Experimental study on heat transfer to supercritical water flowing in 1- and 4-m-Long Vertical Tubes", Proc. GLOBAL'05, Tsukuba, Japan, Oct. 9–13, Paper No. 518, 2005

Koshizuka, S., and Oka, Yo., "Computational analysis of deterioration phenomena and thermal-hydraulic design of SCR, Proceedings of the 1st International Symposium on Supercritical Water-Cooled Reactor Design and Technology (SCR-2000), Paper No. 302, 2000

Krasnoshchekov, E. A., and Protopopov, V. S., "Experimental study of heat exchange in carbon dioxide in the supercritical range at high temperature drops", *Teplofizika Vysokikh Tempraturi* (High Temp.), Vol. 4, No. 3, 1966

Kuang, B., Zhang, Y., and Cheng, X., "A new, wide-ranged heat transfer correlation of water at supercritical pressures in vertical upward ducts, NUTHOS-7, Seoul, Korea, 2008

Löwenberg, M., Starflinger, J., Laurien, E., and Schulenberg, T., "A look-up table for heat transfer of supercritical water", Proc. GLOBAL 2005, Paper No. 037, 2005, pp. 1–6

Löwenberg, M., Starflinger, J., Laurien, E., Class, A., and Schulenberg, T., "Supercritical heat transfer in vertical tubes": A Look-up table, *Progress in Nuclear Energy*, Vol. 50, 2008, pp. 532−538

Mokry, S., Gospodinov, Ye., Pioro, I., and Kirillov, P., "Supercritical water heat-transfer correlation for vertical bare tubes", Proceedings of the ICONE-17, Brussels, Belgium, July 12-16, Paper # 76010, 2009a, 8 pages

Pioro, I.L. 2010, Private communication

Seider, N. M., and Tate, G. E., "Heat transfer and pressure drop of liquids in tubes", *Ind. Eng. Chem.* 28 (12), 1936, pp. 1429–1435

Schmidt, K., Warmetechnische Untersuchungen an hoch belasteten kesselheizffachen (in German), SCHT in water cooled tubes with data graphs, in German, 1959

Swenson, H.S., Carver, J.R., and Kakarala, C.R., Heat transfer to supercritical water in smooth-bore tubes, *J. of Heat Transfer*, *Trans. ASME Series C*, 87 (4), 1965, pp. 477–484

Thom, J.R.S., Walker, W.M., Fallon, T.A., and Reising, G.F.S., "Boiling in sub-cooled water during flow up heated tubes or annuli", *Proc. Inst. Mech. Eng*., Manchester, 1965

Watts, M. J., and Chou, C-T., "Mixed convection heat transfer to supercritical pressure water", Proc. 7th, IHTC, Munich, Germany, 1982, pp. 495–500

Zahlan, H., Groeneveld, D.C., Tavoularis, S., "Look-up table for trans-critical heat transfer", the 2nd Canada-China Joint Workshop on Supercritical Water-Cooled Reactors (CCSC-2010), Toronto, Canada, April 25-28, 2010, 18 pages

Zahlan, H., Groeneveld, D.C., Tavoularis, S., S. Mokry and I. Pioro "Assessment of supercritical heat transfer prediction methods", to be presented at the 5th Int. Sym. SCWR (ISSCWR-5), Vancouver, British Columbia, Canada, March 13-16, 2011, 20 pages

Table 1 The 2010-SCHT water data compilation

Database source	Number of references	Number of data after screening	Data availability
UO	28	6024	Tables and graphs
SJTU	11	7168	Tables and graphs
Stuttgart U	15	2936	Tables and graphs
UOIT	20	8125	Tables and graphs
Combined compilation for all databases			
Number of data before screening	36030	Number of data after screening	24253

Table 2 Overall average and rms errors in the three supercritical sub-regions

Correlation	Liquid-like region		Gas-like region		Close to CP or PC point	
	e_A (%)	e_{RMS} (%)	e_A (%)	e_{RMS} (%)	e_A (%)	e_{RMS} (%)
Bishop et al. (1965)	5	28	5	20	23	31
Swenson et al. (1965)	1	31	-16	21	4	23
Krasnochekov et al. (1967)	18	40	-30	32	24	65
Watts and Chou (1982), Normal	6	30	-6	21	11	28
Watts and Chou (1982), Deter.	2	26	9	24	17	30
Griem (1996)	2	28	11	28	9	35
Jackson (2002)	15	36	15	32	30	49
Mokry et al. (2008)	-5	26	-9	18	-1	17
Kuang et al. (2008)	-6	27	10	24	-3	26
Cheng et al. (2009)	4	30	2	28	21	85
Gupta et al. (2010)	-26	33	-12	20	-1	18
Koshizuka and Oka (2000)	26	47	27	54	39	83
Hadaller and Banerjee (1969)	34	53	14	24	-	-
Sieder and Tate (1936)	46	65	97	132	-	-
Dittus-Boelter (1930)	24	44	90	127	-	-
Gnielinski (1976)	10	36	99	139	-	-

Table 3 Error bands for the best correlations for the combined databases at the three SCHT regions

Error band for 15283 data points	Percentage of data predicted by a correlation, %		
	Mokry et al. (2008)	Gupta et al. (2010)	Swenson et al. (1965)
Near CP region			
e_{10}	46	50	44
e_{20}	79	78	71
e_{30}	92	91	86
e_{50}	99	98	95
Error band for 4386 data points	**Mokry et al. (2008)**	**Watts & Chou (1982), DHT**	**Kuang et al. (2008)**
High density state region (liquid-like region)			
e_{10}	41	28	33
e_{20}	64	57	59
e_{30}	79	79	79
e_{50}	94	95	94
Error band for 4584 data points	**Mokry et al. (2008)**	**Gupta et al. (2010)**	**Bishop et al. (1965)**
Low density state region (gas-like region)			
e_{10}	47	35	45
e_{20}	79	71	75
e_{30}	92	88	89
e_{50}	99	98	97

DHT deteriorated heat transfer

Table 4 Range of parameters and grid points of the trans-critical LUT

Parameter	Parameter range and table grid points							
P (kPa)	19000	20000	21000	22000	22500	23000	24000	25000
	26000	28000	30000	-	-	-	-	-
G (kg m^{-2} s^{-1})	100	200	400	700	1000	1500	2000	3000
	5000	-	-	-	-	-	-	-
ΔT_W (K)	10	20	50	100	200	300	400	500
H_b (kJ/kg)	1000	1400	1600	1800	1900	2000	2050	2100
	2150	2200	2250	2300	2400	2500	2600	2700
	3000	-	-	-	-	-	-	-

Table 5 Parameter range for different LUTs

LUT	*P*, kPa	*G*, kg/m^{2}s	X_{th} (-)	H_b, kJ/kg
2005 CHF-LUT	100–21,000	0–8,000	-0.5–1.0	21–2,800
2003 FB-LUT	100–20,000	0–7,000	-0.2–2.0	21–2,800
Current subcritical LUT	19,000–22,000	100–5,000	-6.25–6.11	1,000–3,000

Table 6 Section of the skeleton table: *HTC* = f (*P* = 21 MPa, *G* = 1000 kg/m^{2}s, ΔT_w, H_b)

P	*G*	ΔT_w	Bulk enthalpy, kJ/kg																
kPa	kgm^{-2}s^{-1}	K	1000	1400	1600	1800	1900	2000	2050	2100	2150	2200	2250	2300	2400	2500	2600	2700	3000
			HTC, kW/m^{2}K																
21000	1000	10	11.89	13.21	14.85	9.04	4.25	6.04	7.01	8.02	9.08	10.18	11.31	12.49	15.42	18.36	14.40	11.58	7.17
21000	1000	20	11.91	13.12	14.22	5.48	2.93	4.16	4.83	5.52	6.25	7.01	7.79	8.60	11.82	15.05	12.47	10.45	6.88
21000	1000	50	11.91	12.37	3.20	3.00	1.72	2.45	2.85	3.26	3.69	4.13	4.59	5.07	7.88	10.69	9.46	8.40	6.20
21000	1000	100	11.68	1.87	1.68	1.96	1.16	1.64	1.91	2.18	2.47	2.77	3.08	3.40	5.63	7.87	7.25	6.70	5.46
21000	1000	200	1.01	0.94	1.06	1.35	0.81	1.15	1.33	1.52	1.73	1.93	2.15	2.37	4.01	5.65	5.37	5.13	4.58
21000	1000	300	0.59	0.73	0.87	1.13	0.68	0.97	1.12	1.29	1.45	1.63	1.81	2.00	3.32	4.65	4.48	4.35	4.07
21000	1000	400	0.48	0.64	0.78	1.03	0.62	0.88	1.02	1.17	1.32	1.48	1.65	1.82	2.93	4.05	3.95	3.86	3.72
21000	1000	500	0.42	0.59	0.73	0.97	0.58	0.83	0.96	1.10	1.25	1.40	1.55	1.72	2.68	3.65	3.58	3.53	3.47
21000	1500	10	16.37	18.23	20.59	13.04	6.13	8.72	10.11	11.58	13.10	14.68	16.32	18.02	22.25	26.49	20.77	16.71	10.34
21000	1500	20	16.39	18.11	19.71	7.91	4.22	6.00	6.96	7.97	9.02	10.11	11.24	12.40	17.06	21.71	17.99	15.07	9.92
21000	1500	50	16.38	17.06	4.61	4.33	2.49	3.54	4.10	4.70	5.32	5.96	6.62	7.31	11.37	15.42	13.65	12.12	8.95
21000	1500	100	16.08	2.70	2.42	2.83	1.67	2.37	2.75	3.15	3.57	4.00	4.44	4.90	8.13	11.35	10.45	9.66	7.87
21000	1500	200	1.46	1.36	1.53	1.95	1.16	1.66	1.92	2.20	2.49	2.79	3.10	3.42	5.79	8.16	7.75	7.40	6.61
21000	1500	300	0.86	1.05	1.25	1.64	0.98	1.40	1.62	1.85	2.10	2.35	2.61	2.89	4.80	6.71	6.47	6.28	5.87
21000	1500	400	0.69	0.92	1.12	1.48	0.89	1.27	1.47	1.69	1.91	2.14	2.38	2.62	4.23	5.84	5.69	5.58	5.37
21000	1500	500	0.61	0.86	1.05	1.40	0.84	1.20	1.39	1.59	1.80	2.02	2.24	2.47	3.87	5.26	5.16	5.09	5.00
21000	2000	10	20.55	22.94	25.99	16.91	7.95	11.31	13.12	15.01	16.99	19.04	21.17	23.37	28.86	34.36	26.94	21.68	13.41
21000	2000	20	20.58	22.78	24.88	10.26	5.47	7.78	9.03	10.34	11.70	13.11	14.58	16.09	22.12	28.16	23.33	19.55	12.87
21000	2000	50	20.58	21.47	5.98	5.62	3.23	4.59	5.32	6.09	6.90	7.73	8.59	9.48	14.74	20.00	17.70	15.72	11.61
21000	2000	100	20.19	3.51	3.14	3.67	2.16	3.08	3.57	4.09	4.62	5.18	5.76	6.36	10.54	14.72	13.56	12.53	10.21
21000	2000	200	1.90	1.76	1.98	2.53	1.51	2.15	2.49	2.85	3.23	3.62	4.02	4.44	7.51	10.58	10.06	9.60	8.58
21000	2000	300	1.11	1.37	1.62	2.12	1.27	1.81	2.10	2.40	2.72	3.05	3.39	3.74	6.22	8.70	8.39	8.14	7.62
21000	2000	400	0.89	1.20	1.45	1.93	1.16	1.65	1.91	2.19	2.47	2.77	3.08	3.40	5.49	7.58	7.38	7.23	6.97
21000	2000	500	0.79	1.11	1.36	1.82	1.09	1.55	1.80	2.06	2.33	2.62	2.91	3.21	5.02	6.83	6.69	6.60	6.49

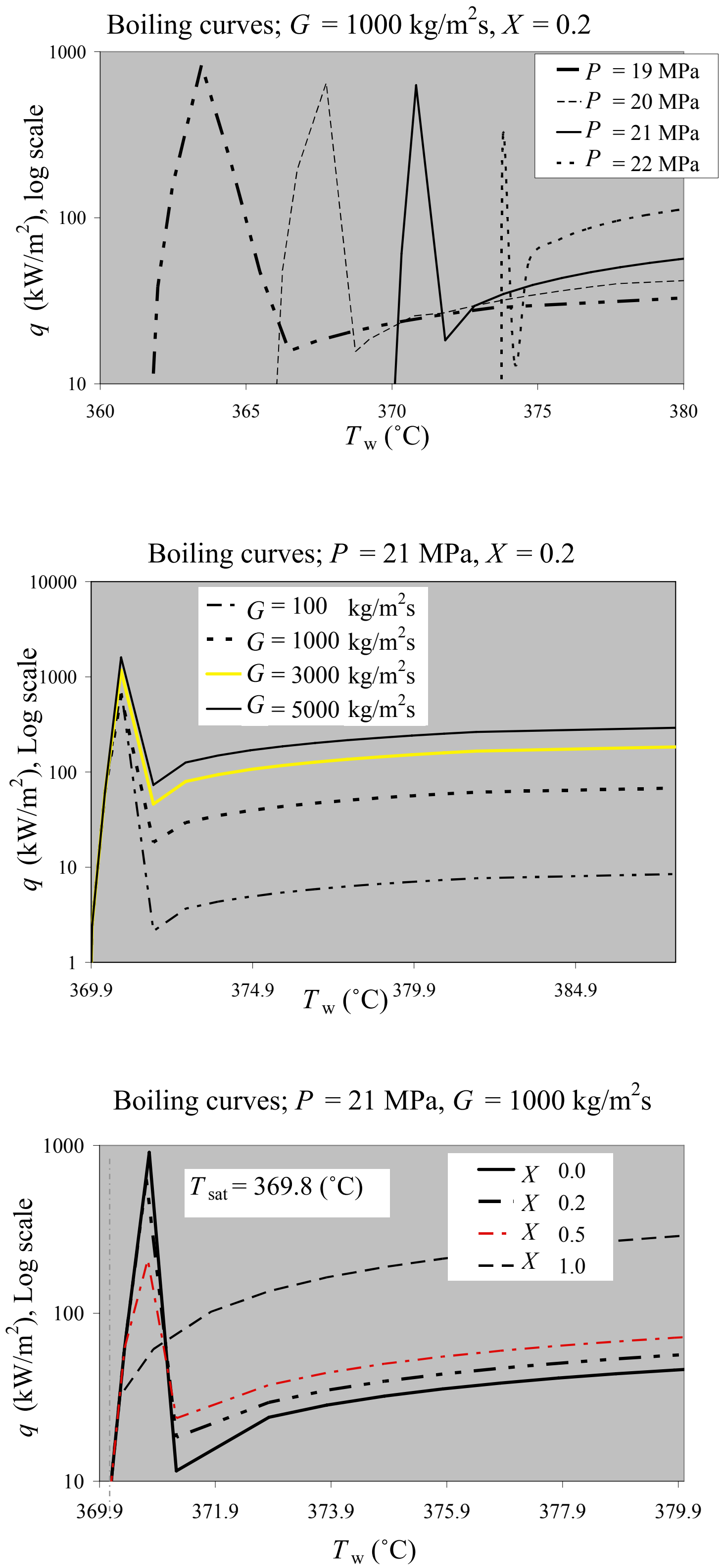

Figure 1 Sets of boiling curves for the range of flow conditions predicted by the sub-critical skeleton table.

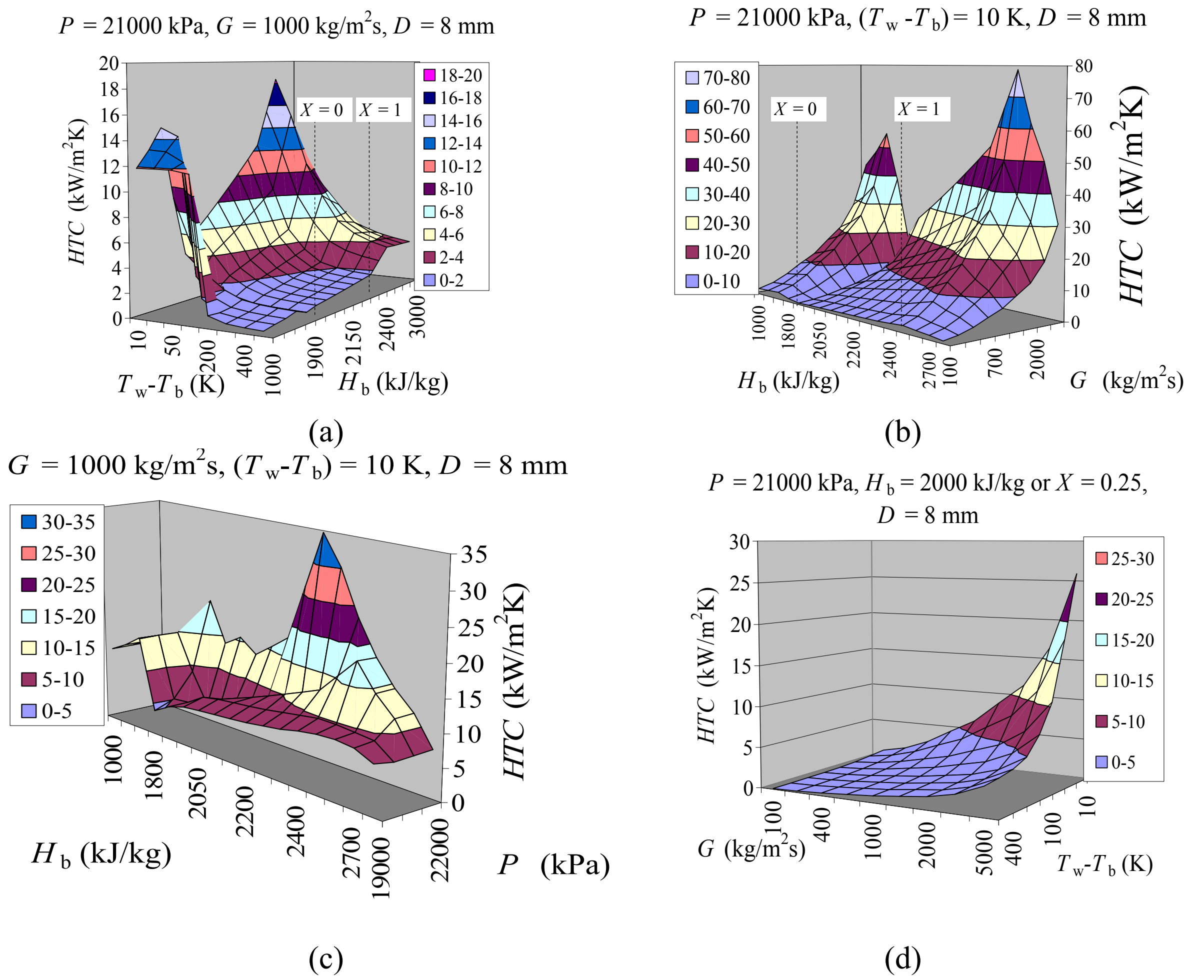

Figure 2 Parametric trends of the subcritical skeleton table.

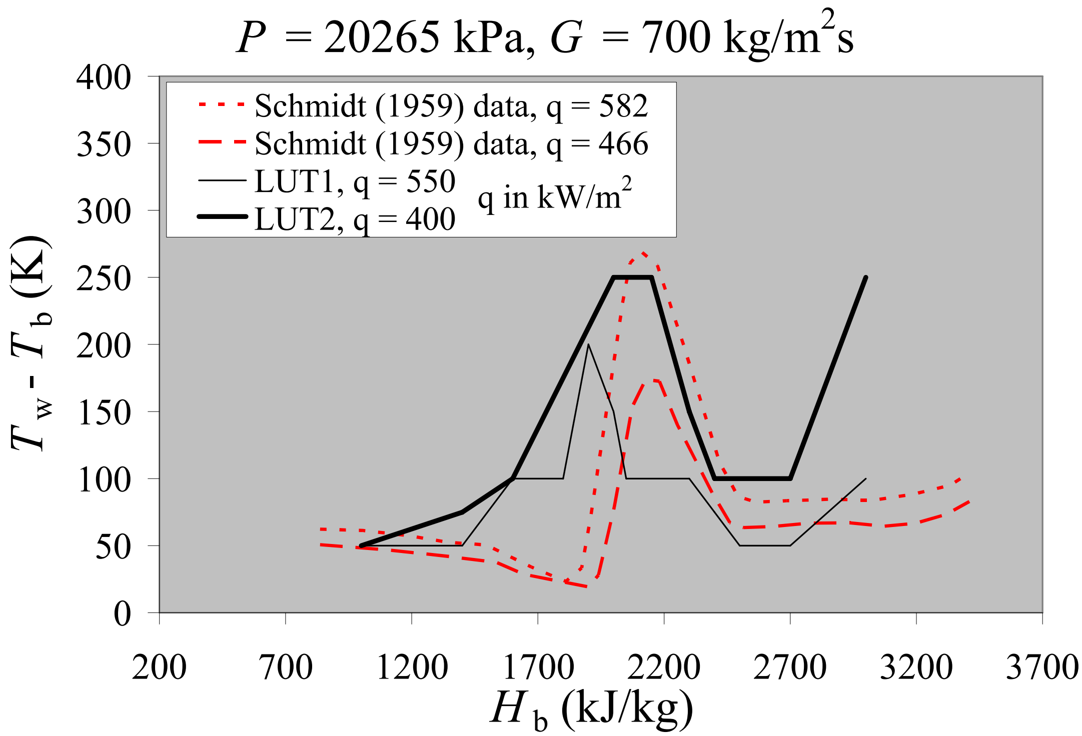

(a)

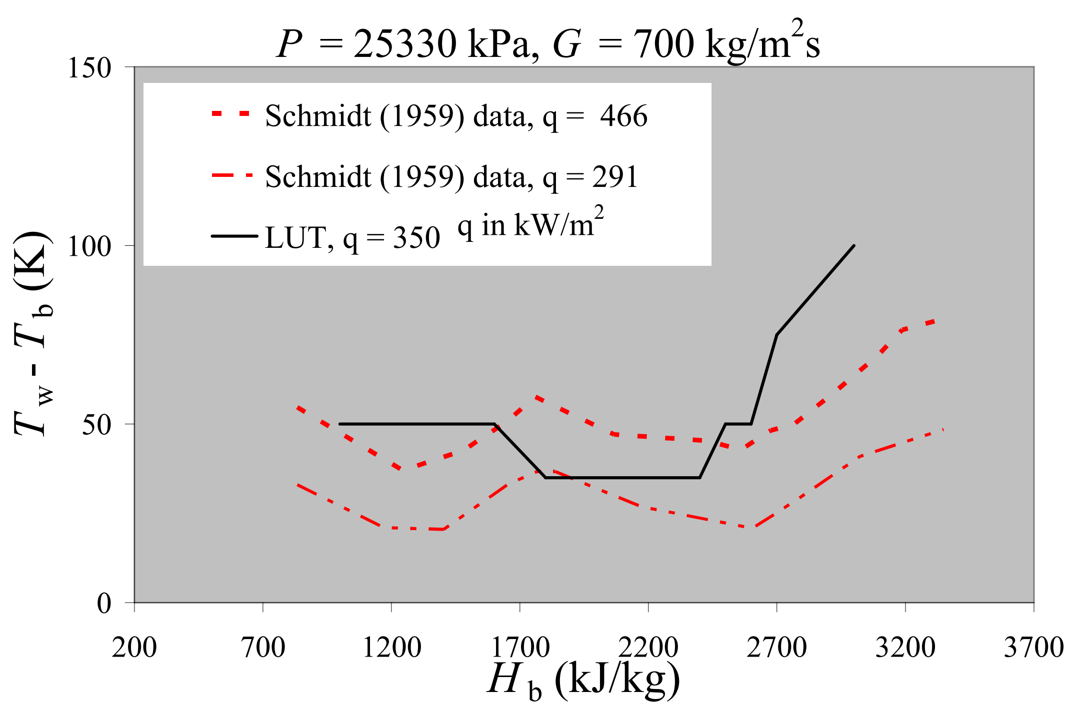

(b)

Figure 3 Comparison of parametric trends of the skeleton table and data by Schmidt (1959).